

Original

## Pulmonary responses in rat lungs after intratracheal instillation of 4 crystal forms of titanium dioxide nanoparticles

Takami Okada<sup>1</sup>, Akira Ogami<sup>1</sup>, Byeong Woo Lee<sup>1</sup>, Chikara Kadoya<sup>1</sup>, Takako Oyabu<sup>1</sup> and Toshihiko Myojo<sup>1</sup>

<sup>1</sup>Institute of Industrial Ecological Sciences, University of Occupational and Environmental Health

**Abstract: Objective:** Titanium dioxide nanoparticles are widely used as UV filters in cosmetics and as a photocatalyst. We evaluated pulmonary responses to different crystal forms of TiO<sub>2</sub> nanoparticles. **Methods:** We used 4 different TiO<sub>2</sub> samples with similar specific surface areas (anatase, rutile, amorphous, and P25). Each sample was suspended in distilled water and intratracheally instilled to male Wister rats at the dose of 1 mg per rat. Five rats per group were sacrificed at 3 days, 1 month, and 6 months after instillation, and bronchoalveolar lavage fluid was collected from the right lung to determine the total cell count and polymorphonuclear cell (PMN) counts. The left lung tissues were stained with hematoxylin and eosin for the evaluation of inflammation and with elastica van Gieson for the evaluation of collagen deposition. **Results:** The total cell counts and PMN counts of the amorphous and P25 of four samples showed a significant increase compared with the control group at 3 days after instillation. The inflammation rate of P25 also showed a significant increase compared with controls at 3 days. The collagen deposition rate in the alveolar duct of P25 increased significantly compared with controls from 3 days to 6 months. The other samples showed a mild response after instillation. **Conclusion:** Although the TiO<sub>2</sub> nanoparticles used in this study had similar specific surface areas, there were different inflammatory responses in the rat lungs. Other factors, such as different production processes or the surface activities of particles, may have been responsible for the dif-

ferent responses.

(J Occup Health 2016; 58: 602-611)

doi: 10.1539/joh.16-0094-OA

**Key words:** Anatase, Nanoparticles, Pulmonary response, Rutile, Titanium dioxide

### Introduction

With recent advances in material science, workers are now handling new materials that did not previously exist, such as engineered nanomaterials. The post-exposure biological effects of such new materials are of serious concern. The mass concentration of aerosolized dust particles is used as the basic index for the threshold exposure limits of materials, but the biological effects of engineered nanomaterials are thought to be different from those of the corresponding bulk materials that are subject to the present regulations. Prior to any toxicity studies of these nanomaterials, the following physicochemical properties of the samples should be identified: particle size and/or size distribution, specific surface area, crystal structure/crystallinity, aggregation status, surface coatings, surface reactivity, method of synthesis, and purity of sample<sup>1</sup>.

Titanium dioxide (TiO<sub>2</sub>) nanoparticles are widely used as photocatalysts and in cosmetics. Pigment grade TiO<sub>2</sub> seems to be a less harmful substance, but there is some concern about its pulmonary toxicity and dermal absorption<sup>2</sup>. Titanium dioxide nanoparticles are commercially produced from TiCl<sub>4</sub> using hydro-carbon assisted flame synthesis, i.e., the so-called “chloride process.” In Japan, TiO<sub>2</sub> nanoparticles are also produced by the so-called “sulfate process,” where the hydrolysis of the titanyl sulfate (TiOSO<sub>4</sub>) yields hydrated titanium dioxide and then heating of the solid in a furnace evaporates the water and decomposes any remaining sulfuric acid in the solid. Crystals of the TiO<sub>2</sub> produced by both methods may also

Received April 8, 2016; Accepted August 7, 2016

Published online in J-STAGE September 30, 2016

Correspondence to: T. Okada, Institute of Industrial Ecological Sciences, University of Occupational and Environmental Health, 1-1 Iseigaoka, Yahatanishi-ku, Kitakyushu, 807-8555, Japan (e-mail: okadatakami@me.d.uoeh-u.ac.jp)

**Table 1.** Physicochemical properties of TiO<sub>2</sub> particles

Sample	Company	Manufacturing process	BET surface area (m <sup>2</sup> /g)	Sauter mean diameter* (nm)	Crystallite size (nm)		Hydrodynamic mean diameter ** (nm)
					Anatase	Rutile	
Anatase AMT-400	TAYCA corporation	Sulfate process	102	15	16.9	–	737
Rutile MT-150W	TAYCA corporation	Sulfate process	102	14	–	15.5	348
Amorphous	Wako Pure Chemical Industries	NA	110	14	6.1	–	226
P25	EVONIK Industries	Chloride process	53.8	28	23.5	35.9	205

\*Sauter diameter =  $6 / (\text{density of materials} \times \text{surface area})$

\*\*Cumulants mean size of suspensions in distilled water measured by DLS (Malvern Zetanalyzer S)

be coated with another substance, such as aluminum oxide or silica<sup>3</sup>). Several other methods have also been developed recently to synthesize TiO<sub>2</sub> nanoparticles by either pyrolysis reactions or hydrolysis methods<sup>4</sup>).

Jiang et al.<sup>5</sup>) measured the levels of reactive oxygen species (ROS) produced by various types of gas-phase-synthesized TiO<sub>2</sub> particles *in vitro*, and reported that 30-nm particles had the highest ROS production per unit surface area, and that the ROS production level decreased depending on the crystal form in the following order when the particle sizes were the same: amorphous, anatase, anatase/rutile, and rutile.

Both anatase and rutile TiO<sub>2</sub> particles are widely used. An inhalation exposure test using rats performed by Ferin and Oberdorster<sup>6</sup>) demonstrated no differences in biological responses between the rutile and the anatase nanoparticles. Afterwards, another inhalation exposure test showed that more severe pulmonary inflammatory responses were induced by ultrafine (nano-size) TiO<sub>2</sub> particles than by larger (submicron-size) TiO<sub>2</sub> particles, and the biological effects of nanoparticles have since become a serious concern<sup>7</sup>).

Evaluation of the pulmonary toxicity of airborne nano-materials involves exposing animals to nanomaterials by inhalation (OECD Test Guideline 412, 413). Bermudez et al.<sup>8</sup>) assessed pulmonary responses of rats, mice, and hamsters to inhaled P25 nanoparticle aerosols, in which pulmonary inflammation and retardation of particle clearance was evident in rats and mice exposed to 10 mg/m<sup>3</sup> for 13 weeks. However, many institutes are unable to easily design and conduct inhalation tests of any modified or newly developed products.

Intratracheal instillation is a technique that is appropriate for evaluating the possible hazards of nanomaterials, but it is less appropriate for deriving threshold values and quantitatively assessing risk. Warheit et al.<sup>9,10</sup>) proposed pulmonary bioassay bridging studies between inhalation

exposure and intratracheal instillation. A bridging study can serve as screening when assessing the safety of newly developed or modified samples compared with reference samples<sup>11</sup>).

In this study, we intratracheally administered 4 kinds of nano-size TiO<sub>2</sub> samples with similar specific surface areas (100 m<sup>2</sup>/g) to male Wistar rats at the dose of 1 mg. To evaluate the difference of toxicity among the samples with different crystal forms, the numbers of total cells and polymorphonuclear cells (PMN) counts in the bronchoalveolar lavage fluid (BALF) of each right lung were determined to measure inflammatory changes, and the left lung tissue was used for histopathological examinations.

## Materials and Methods

### Titanium Dioxides

We used four nano-size TiO<sub>2</sub> samples: anatase, rutile, amorphous, and P25. Details of the samples are shown in Table 1. The samples of anatase and rutile were produced by the “sulfate process” without any surface treatment, as per the manufacturer’s information. The sample of amorphous was a chemical supply and there was no information about its production. The P25 was synthesized by the “chloride process” and we used a de facto standard sample for toxicity of nano-size TiO<sub>2</sub> samples. These samples were gifts from the manufacturers except for the sample of amorphous.

The specific surface areas of these four samples were measured by a BET apparatus. Based on the BET theory<sup>12</sup>), the specific surface areas were measured by N<sub>2</sub> absorption onto the samples using a Quantachrome Instruments NOVA-1200 (Boynton Beach, FL, USA) by the Ube Scientific Analysis Laboratory (Ube, Japan). The specific surface areas of the samples and calculated Sauter diameters are shown in Table 1.

Powder XRDs for the TiO<sub>2</sub> samples were carried out by

Rigaku RINT-TTR III (Rigaku Co., Tokyo), of which the wavelength of X-ray (Cu K $\alpha$ ) operated at 300 mA and 50 kV was 0.154 nm. The XRD patterns were obtained at a scanning rate of 5 deg/min over a range of 5 to 100 deg (2  $\theta$ ) by the Ube Scientific Analysis Laboratory (Ube, Japan). Microphotographs of the samples were observed by a scanning electron microscope (Hitachi S-4500, Tokyo, Japan).

#### *Preparation of Sample Suspensions*

Bulk TiO<sub>2</sub> powder was dispersed in sterile purified water by sonication for total 15 min using an ultrasonic sonicator (Sonifier 250, Branson, USA) to minimize the particle diameter in distilled water without any dispersant. The size distributions of the TiO<sub>2</sub> particles in the suspensions were measured by the dynamic light scattering method (DLS, Zetasizer Nano S, Marvern). All the samples showed that the majority of the particles in the suspensions were agglomerates but we did not remove these particles in order to keep the values of specific surface area measured by the BET method.

#### *Animals*

Male Wistar rats (8 weeks old) were purchased from Kyudo Co., Ltd. (Kumamoto, Japan). The animals spent one week in the Laboratory Animal Research Center of the University of Occupational and Environmental Health with a commercial diet and water provided ad libitum. The rat body weights were 320 $\pm$ 15 g at the start of exposure (9 weeks old). All procedures involving the handling of animals followed the Japanese Guide for the Care and Use of Laboratory Animals as approved by the Animal Care and Use Committee, University of Occupational and Environmental Health, Japan.

#### *Intratracheal Instillation*

Rats were instilled at a dose of 1 mg (3.1 mg/kg) for all samples. That dose is between the 1 mg/kg and 5 mg/kg doses chosen by Warheit et al.<sup>10</sup>. In our previous report<sup>13</sup>, the intratracheal instillation of 1 mg/rat TiO<sub>2</sub> (P90, Evonik) induced a moderate and transient inflammation in rat lung, while 0.2 mg/rat did not. The TiO<sub>2</sub> concentration in the instillation liquid was adjusted to 2.5 mg/ml of TiO<sub>2</sub> nanoparticles in distilled water. The sample suspension (0.4 ml) was intratracheally instilled once to diethylether anesthetized animals by a syringe through a catheter inserted into the airway. A control group was exposed to distilled water. The intratracheal instillations were conducted twice, that is, the anatase group and rutile group, or the amorphous group and P25 group with each control group, but administered by the same operator.

#### *Bronchoalveolar lavage fluid (BALF)*

Five rats for each dose were dissected at 3 days, 1 month, and 6 months after instillation. The rats were sac-

rificed by exsanguination from the heart under deep anesthesia by intraperitoneal injection of pentobarbital, and then the lungs were removed from the chest cavity. BALF was collected by inserting a cannula into the right lung via the respiratory tract, with the left main bronchus clamped, and pouring in a physiological saline (5 to 10 mL each). Fifty ml of BALF was centrifuged (1500 rpm; 10 min) to separate the cellular components. After 1 mL of buffer was added and stirred thoroughly, they were examined for macrophages and neutrophils (cell/ $\mu$ L) with an automatic blood cell counter (Celltac MEK 5204 Nihon Koden, Tokyo). The results were used as the total number of cells in the BALF.

From the above samples, smears were prepared on glass slides by the CytoSpin method and stained by a Diff-Quik kit (Sysmex Co., Kobe, Japan). These slides were observed by an optical microscope at  $\times$ 400 magnification; 200 cells per slide were differentially counted and the percentage of neutrophils was calculated. The alveolar macrophages (AM) and PMN in the BALF were identified by their shape. The number of PMN in the BALF was obtained by multiplying the percentage of PMN by the total number of cells.

#### *Histopathology of rat lungs*

The left lung of each rat (the clamped side in the BALF collection) was fixed with 10% buffered formalin at 25 cmH<sub>2</sub>O pressure overhead. Paraffin sections of the left lung (3  $\mu$ m thickness) were stained with hematoxylin-eosin (HE) and elastica van Gieson (EVG) by Hist Science Laboratory Co., Ltd. (Tokyo, Japan).

##### 1) Point counting method for HE staining

After each specimen was stained, six digital images of each lung section, focusing mainly on the alveoli and excluding the large vessels and trachea, were photographed with a digital camera (DS-5M; Nikon Instech Co. Ltd., Kanagawa, Japan) under light microscopy at  $\times$ 100 magnification. In order to eliminate measurer bias, a third person randomly assigned numbers from 1 to 90 to microscope photographs (3 doses  $\times$  5 animals  $\times$  6 photographs) per time point and returned them to the measurer. After completion of measuring, the photographs were returned to the original order by using a conversion table. A 300-point grid was placed over each image on a computer screen and the measurer examined pulmonary inflammation at each time point using the point counting method (PCM)<sup>14-16</sup>. The accumulation of macrophages and PMN was counted mainly as inflammatory change. The rate of points of inflammation was calculated, as shown below:

$$I = X/300$$

where I is the inflammation rate and X is the number of inflammation points among 300 points.

##### 2) Point counting method for EVG staining

To evaluate the extent of fibrosis, digital images were taken of sections stained by the elastica van Gieson

method. Two images were captured by  $\times 400$  magnification at the alveolar duct region and the pleura region, and each image was recaptured through polarized light. The birefringent areas (collagen positive) and interstitium areas were analyzed by the PCM. The rate of collagen deposits (points where there were birefringent areas) for each section was calculated as follows:

$$CD = (\text{Number of birefringent points in parenchyma}) / (\text{total number of points in the lung parenchyma})$$

where CD is the collagen deposited rate.

#### Statistical analysis

Results are presented as means  $\pm$  standard deviation. The results were compared with the Mann-Whitney U-test, with differences of  $p < 0.05$  or less considered to be statistically significant. Statistical analysis was performed using IBM SPSS Statistics 19 (IBM Corp., Armonk, NY).

## Results

X-ray diffraction patterns and scanning electron microscope images of the 4 samples are shown in Fig. 1. Fig. 1A and 1B show that there were  $\text{TiO}_2$  nanoparticles in the anatase (the major diffraction angle of  $25.3^\circ$ ) and in the rutile (the major diffraction angle of  $27.4^\circ$ ), respectively. Fig. 1C shows amorphous particles, with a broad peak of the anatase crystallites. The P25 nanoparticles contained both anatase and rutile crystallites; the amount of anatase was larger than rutile, indicated by a 10-fold higher X-ray diffraction peak (Fig. 1D). The crystallite sizes of the  $\text{TiO}_2$  using the Scherer equation were estimated as shown in Table 1.

The BET surface areas of the  $\text{TiO}_2$  nanoparticles of both the anatase and rutile were  $102 \text{ m}^2/\text{g}$ , while those of the amorphous and P25 were  $110 \text{ m}^2/\text{g}$  and  $53.8 \text{ m}^2/\text{g}$ , respectively. Except for the P25, the BET areas of the  $\text{TiO}_2$  nanoparticle samples were similar. The Sauter diameters, defined as the diameter of equivalent surface sphere, were 14 nm for both the anatase and rutile, 15 nm for the amorphous particles, and 28 nm for the P25. Images of each of the samples are shown in Fig. 1 with the Sauter diameter indicated (white circle).

Hydrodynamic diameters of sample suspensions are shown in Table 1. In the table, we showed the cumulants mean size (nm) of the DLS.

#### Bronchoalveolar lavage fluid (BALF)

The total cell counts and PMN counts in the BALF are shown in Fig. 2A and 2B, respectively. The experiment process was conducted twice, and the differences from the corresponding control groups were examined for statistical significance. The total cell counts 3 days after administration were significantly higher in the group with instillation of amorphous (the amorphous group) and in that with instillation of P25 (the P25 group), whereas the

groups with instillation of anatase or rutile (the anatase or the rutile group) were undistinguishable. There were no significant increases in any sample beyond 1 month after administration.

Similar to the changes in the total cell counts, the PMN counts 3 days after administration were significantly higher in the amorphous group and in the P25 group. Changes were largest in the amorphous group, and then in the P25 group. The rutile group and the anatase group showed similar differences, which were much smaller than those seen in the amorphous group and the P25 group. None of the groups showed significant differences beyond 1 month after administration.

#### Histopathology

HE-stained images of lung tissues 3 days after administration of each nanoparticle sample are shown in Fig. 3. Inflammation was observed in the amorphous group (Fig. 3C) and the P25 group (Fig. 3D); it was particularly severe in the alveolar ducts in the P25 group. Notable inflammation was not observed in Fig. 3A and 3B but macrophages phagocytizing particles are also observed. Gradual alleviation was observed 1 month after administration, and further improvement was seen 6 months after administration (data not shown).

Polarizing light microscopy images of EVG-stained sections of lungs 6 months after administration are shown in Fig. 4. The shiny regions indicate the existence of collagen fibers.

The levels of inflammation in the lung tissues assessed by the point counting method are shown in Fig. 5A. A significant increase was seen only in the P25 group. The P25 group showed the largest change, followed by the amorphous group, the rutile group and then the anatase group. However, such changes were seen only 3 days after instillation, and no significant changes compared with the control group were confirmed in any of the four groups beyond 1 month after instillation.

The level of collagen deposition was assessed by the point counting method (Fig. 5B and C). When the P25 group was compared with the control group, the collagen deposition rates were significantly higher ( $p < 0.01$ ; Mann-Whitney U test) in the alveolar ducts 3 days, 1 month, and 6 months after instillation (Fig. 5B), and in the pleura 3 days after instillation (Fig. 5C). The collagen deposition rates in the pleura in the P25 group 1 month and 6 months after instillation were higher than in the control group but not statistically significant. The rutile group and the anatase group showed significantly higher values than the control group ( $p < 0.05$ ) in the alveolar ducts 3 days after instillation and 1 month after instillation, respectively.

## Discussion

The sizes of the crystallites in the anatase and rutile

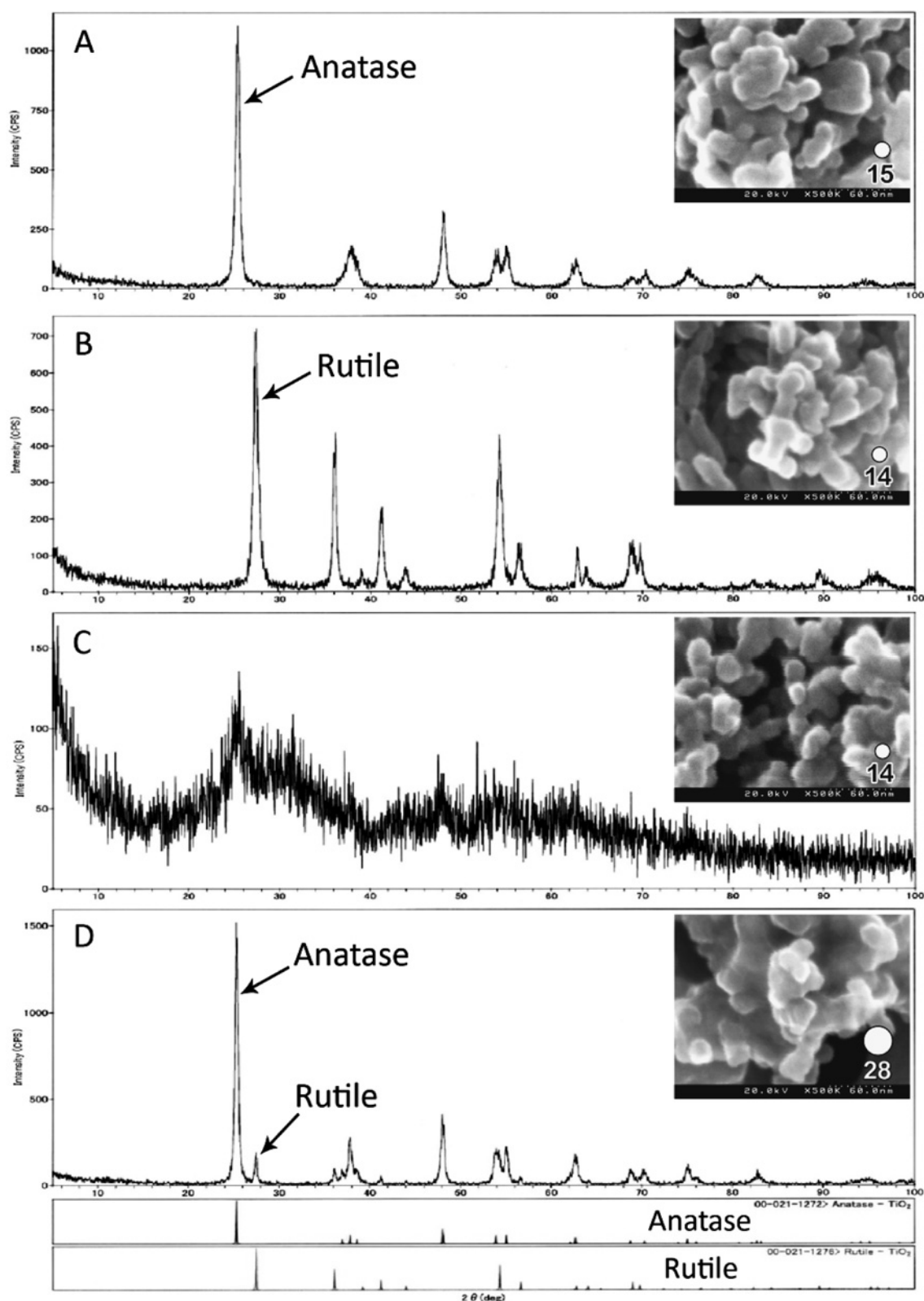


**Fig. 1.** X-ray diffraction analysis (XRD) of  $\text{TiO}_2$  particles. (A) Anatase, (B) Rutile, (C) Amorphous, (D) P25. Scanning electron micrographs of  $\text{TiO}_2$  particles: (A) Anatase, (B) Rutile, (C) Amorphous, (D) P25.

phases were larger than the corresponding Sauter diameters, while those in the amorphous and P25 nanoparticles

were smaller than the corresponding Sauter diameters, as shown in Table 1. These findings suggest that the anatase

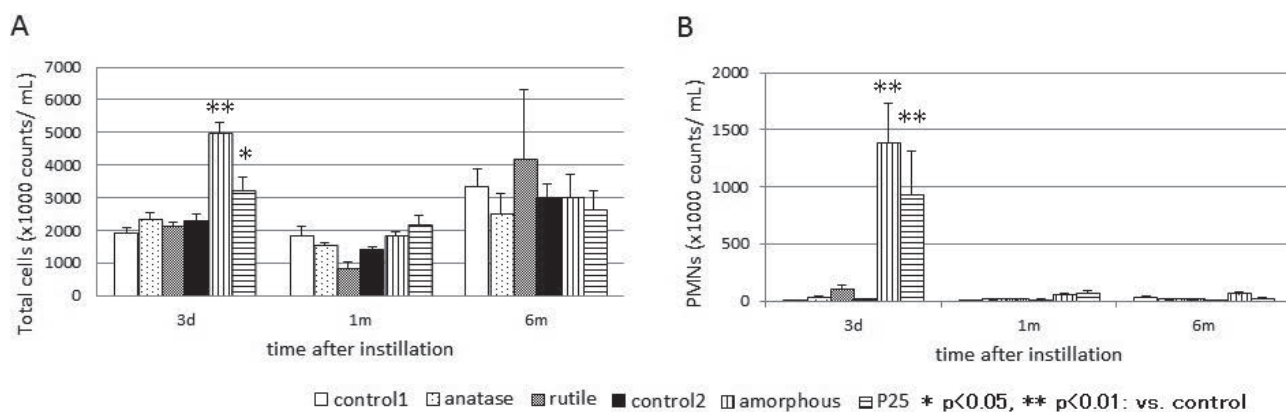


Fig. 2. Total cells counts in BALF (A) and PMN counts in BALF (B).

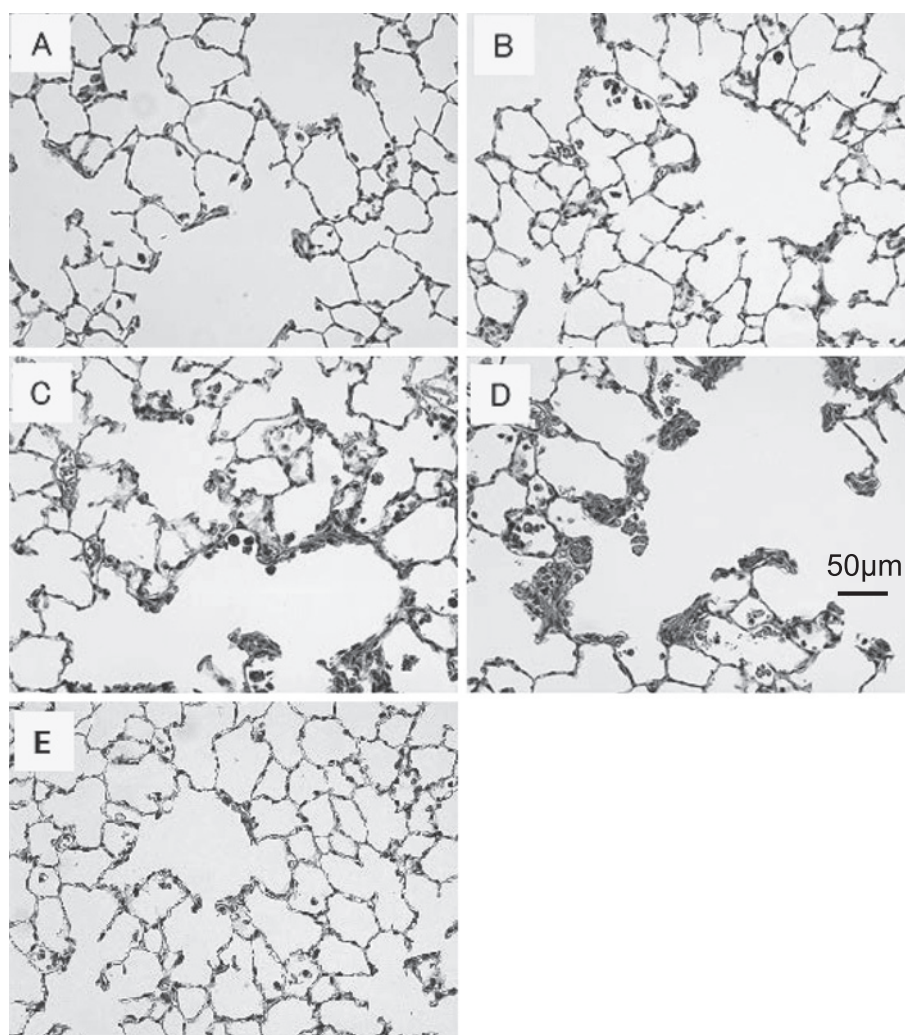
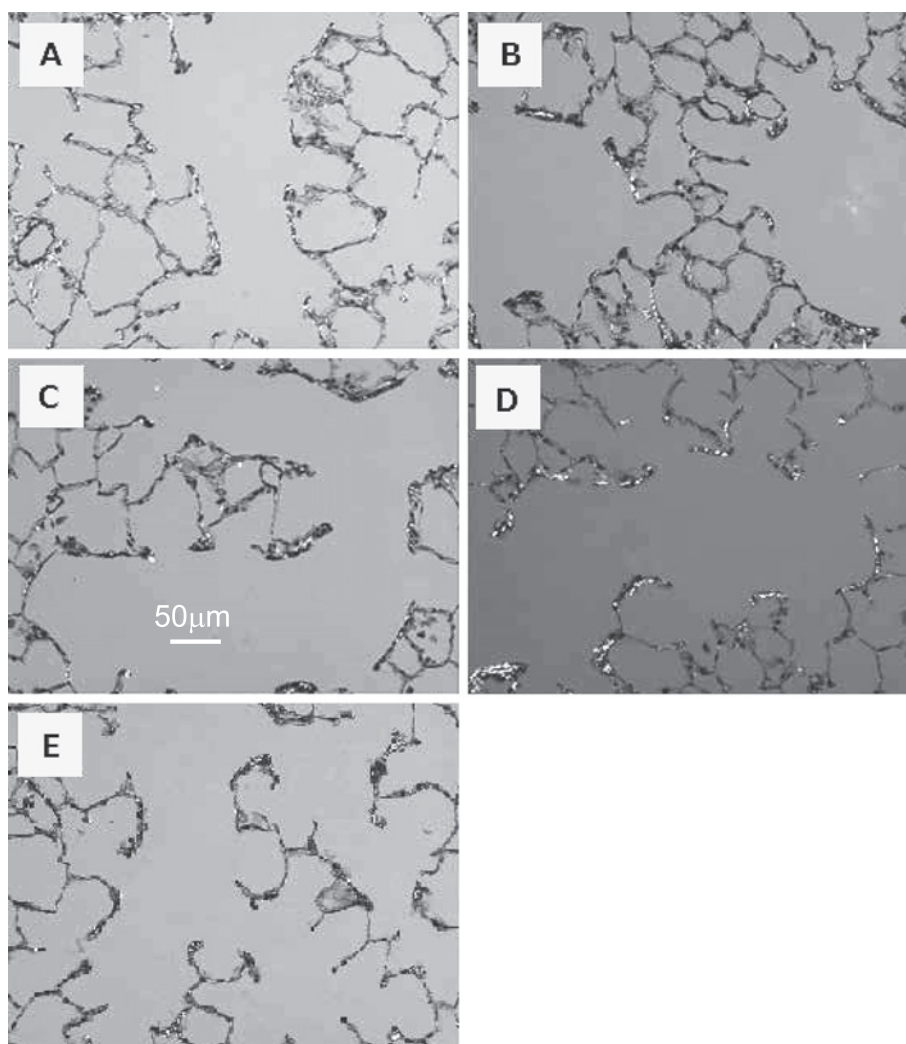


Fig. 3. Representative image of rat lung sections with HE stain at 3 days after intratracheal instillation (x200): (A) Anatase, (B) Rutile, (C) Amorphous, (D) P25, and (E) control.

and rutile samples were agglomerates of monocrystalline primary particles, while the amorphous and P25 samples were partial aggregates wherein crystallites adhere to each

other and the surface area is reduced.

The characteristics of the sample suspensions are important for in vitro and instillation tests. In this study, as



**Fig. 4.** Representative image of rat lung sections with EVG stain at 6 months after intratracheal instillation ( $\times 200$ , polarized): (A) Anatase, (B) Rutile, (C) Amorphous, (D) P25, and (E) control.

we focused on received bulk sample characteristics, such as BET surface areas and XRD, we did not use any dispersants or size control technique of the suspension. Cumulants mean sizes were more than 100 nm, as shown in Table 1.

In our previous study<sup>13</sup>, the suspension of TiO<sub>2</sub> nanoparticles in distilled water were centrifuged for 20 min at 8,900  $\times g$  and then the supernatants were instilled as the samples. The hydrodynamic diameter of well-dispersed TiO<sub>2</sub> nanoparticles was 25 nm measured by DLS.

Warheit et al.<sup>10</sup> measured the hydrodynamic diameter of TiO<sub>2</sub> nanoparticle agglomerates in the suspensions with dispersant (tetrasodium pyrophosphate, 0.1 wt%) and phosphate buffer solution (PBS), of which hydrodynamic diameters were ranging from 130 to 382 nm with dispersant and from 2144 to 2890 nm with PBS and they instilled the sample suspensions with PBS to rats.

Zeta potentials of the samples were not measured in

this study. The zeta potential of P25 with distilled water was +27 mV reported by Rushton et al<sup>17</sup>. Other study reported that the zeta potential of pure anatase nanomaterial with distilled water was +35 mV and that of pure rutile nanomaterial with distilled water was -33 mV<sup>18</sup>. Our previous study<sup>19</sup> showed the zeta potentials tend to be negative for rutile and positive for anatase (both not used in this study) and medium for the amorphous (used in this study) in a buffer solution. So, zeta potentials of the samples with distilled water may be reflected by the crystal forms of the samples.

Bermudez et al.<sup>8</sup> exposed rats (F344), mice (B3C3F1/CrlBR), and hamsters to P25 nanoparticles by inhalation for 13 weeks, and found that the biological effects of P25 inhalation exposure were more prominent in the rats than in the mice and hamsters. When rats were exposed to P25 at the concentration associated with biological effects (10 mg/m<sup>3</sup>, mass median aerodynamic diameter = 1.37  $\mu m$ ),

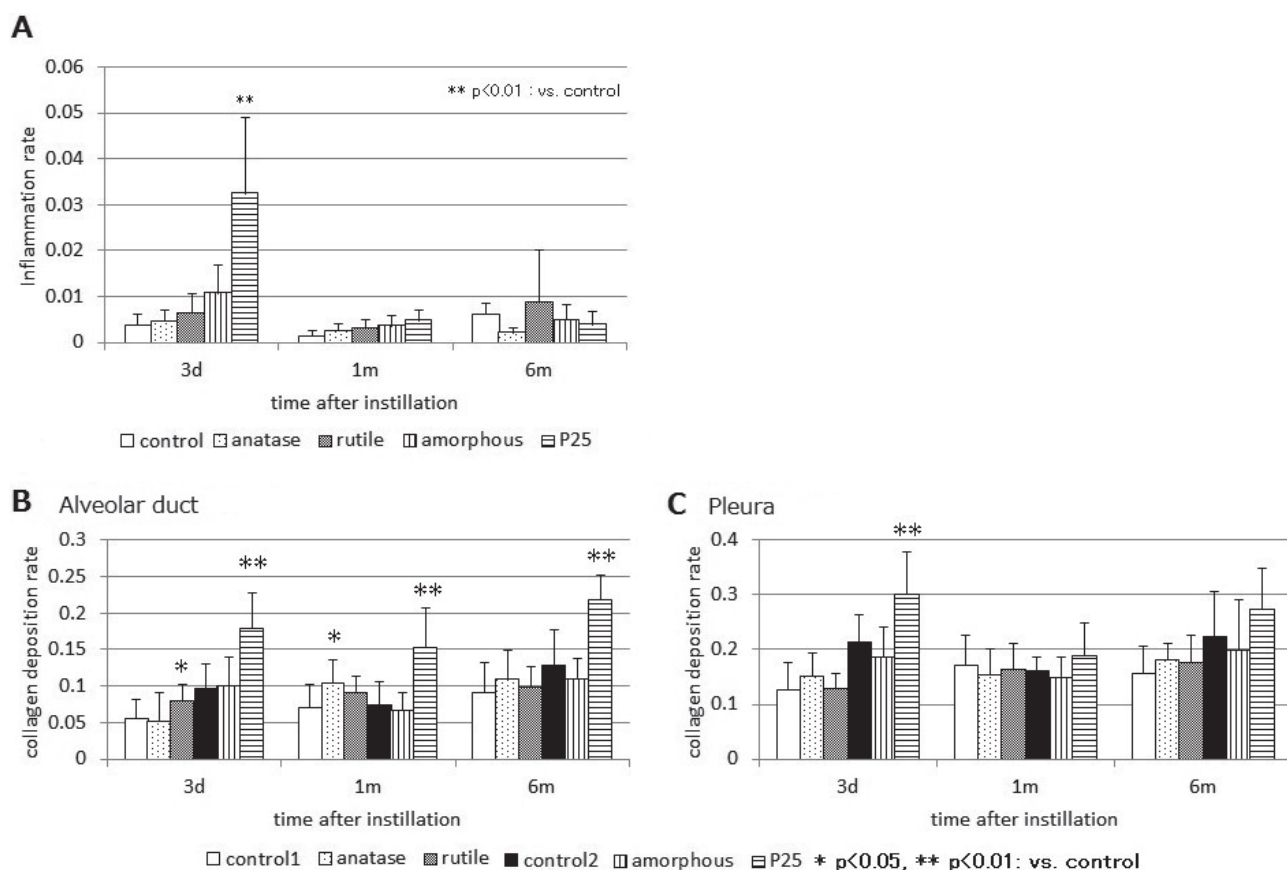


**Fig. 5.** The inflammation area rate (A) by point counting method (PCM) after instillation. In the P25 group, inflammation rate raised significantly with control at 3days after instillation. Collagen deposition rate by point counting method: (B) alveolar duct, and (C) pleura.

the level of deposition in each lung was 2.1 mg. In our previous study<sup>13)</sup>, the average pulmonary retention of TiO<sub>2</sub> was 0.56 mg at 3 days after intratracheal instillation of 1 mg of TiO<sub>2</sub> nanoparticles (P90) and the rest of the TiO<sub>2</sub> was cleared. The retention is close to the amount of pulmonary retention seen after 13 weeks inhalation exposure to P25 particles at a concentration (2 mg/m<sup>3</sup>) that did not cause a biological effect<sup>8)</sup>. In the present study, we found positive biological effects after intratracheal instillation of 1 mg/rat for P25 TiO<sub>2</sub> samples. These biological effects may be enhanced by single bolus dose of the samples by direct injection to lung.

In the present study, we examined pulmonary responses to four crystal forms of TiO<sub>2</sub> nanoparticles with the same doses in both weight and surface area, and found that they caused considerably different levels of inflammation: amorphous>P25>> rutile=anatase, 3 days after administration (see Fig. 2). The inflammation levels were not significantly different beyond 1 month after administration in all conditions. The changes seen 3 days after administration in the amorphous group and the P25 group in the present study (Fig. 2) were in good agreement with the significant increases in total cell count and PMN

count in BALF 3 days after intratracheal instillation of 1 mg of well-dispersed TiO<sub>2</sub> (P90)<sup>13)</sup>.

Höhr et al.<sup>20)</sup> investigated the acute inflammatory response in rat lungs after intratracheal instillation of surface modified (hydrophilic and hydrophobic) fine and ultrafine TiO<sub>2</sub> particles. The responses, such as total cell counts and PMN counts in BALF, were significantly related to the administered surface dose and there were no statistically significant differences between hydrophilic and hydrophobic TiO<sub>2</sub> particles at the dose of 1 mg. Rehn et al.<sup>21)</sup> reported that rats instilled with a single dose of 0.15-1.2 mg of P25 or silanized TiO (hydrophobic surface) nanoparticles showed no signs of inflammation. In contrast, a strong progression in the lung inflammatory response was observed in quartz-exposed rats (0.6 mg).

Warheit et al.<sup>9,10)</sup> reported that transient neutrophil infiltration in the lung of SD rats was observed at a dose of 5 mg/kg but was not observed at a dose of 1 mg/kg after intratracheal exposures to three kinds of TiO<sub>2</sub> made by Du-Pont, but at a dose of 5 mg/kg of P25 a moderate and transient inflammation was observed, although not with 1 mg/kg. They concluded that the ranking of lung inflammation and histopathological responses was Quartz>P25>

newly developed TiO<sub>2</sub> nanoparticles.

Bonner et al.<sup>22)</sup> used a P25-administered group as a reference to examine inter-laboratory differences in the biological effect to compare other types of TiO<sub>2</sub> nanoparticles administered by laryngeal aspiration or tracheal instillation to mice and rats. The measured inflammation due to administered TiO<sub>2</sub> nanoparticles varied depending on the laboratories: some found the severest inflammation with P25 administration, while others did not.

Kobayashi et al.<sup>23)</sup> controlled TiO<sub>2</sub> nanoparticle agglomerates in the suspensions, of which hydrodynamic sizes ranged from 20 nm to 200 nm using dispersant (disodium phosphate, 0.2-1.3 wt%). The authors concluded that there was no clear relationship in pulmonary inflammation among the rats instilled samples with the same primary size but different particle agglomerations.

Warhait et al.<sup>10)</sup> speculated that the difference in inflammatory responses to TiO<sub>2</sub> samples was caused by the production process of P25, which does not include an aqueous or wet surface treatment step to neutralize and remove the acidic chloride ions from the surface of the particles to preserve the photo-chemical activity of the TiO<sub>2</sub>. The difference between the anatase-group and the rutile-group vs. the P25-group in our results supports their speculation that the inflammatory responses to TiO<sub>2</sub> depend on surface activity rather than crystal form.

The most important endpoints that have been associated with exposure to respirable particles include chronic persistent inflammation, fibrosis, and cell proliferation in the lungs and mesothelial lining. All the HE-stained lung specimens showed macrophage phagocytosis of nanoparticles 3 days after instillation (Fig. 3).

In order to quantitatively assess the overall levels of pulmonary inflammation, we employed PCM and examined the images of a considerable lung area of each HE-stained section (Fig. 5A). The changes became smaller in the following order: P25 > amorphous > rutile > anatase. However, such differences were seen only 3 days after instillation, and time-dependent increases in the level of inflammation, as seen after exposure to silica<sup>24)</sup>, were absent. Both the amorphous group and the P25 group showed total cells and PMNs counts increase (amorphous > P25) in Fig. 2 but inflammation level evaluated by PCM was high in the P25 group only as shown in Fig. 5A. From our previous studies<sup>15,16)</sup>, PCM reflects to the inflammatory reaction of the lung section, such as hyperplasia of alveolar cells in addition to the infiltration of macrophages or PMNs. The P25 group may have more inflammatory effect for lung tissue than the amorphous group.

Bermudez et al.<sup>8)</sup> demonstrated that inhalation exposure to P25 (10 mg/m<sup>3</sup>) caused the accumulation of inflammatory cells and thickening of type II cells in the alveolar ducts. Warhait et al.<sup>10)</sup> reported the accumulation of P25-containing macrophages in the lung tissue of a rat exposed to P25 (5 mg/kg) at 3 months post-instillation, al-

though exposure to other TiO<sub>2</sub> nanoparticles produced no adverse pulmonary effects.

After an intratracheal instillation of well-dispersed P90 TiO<sub>2</sub> nanoparticles to rats<sup>13)</sup>, accumulations of alveolar macrophages, which phagocytosed the particles, were observed from the terminal bronchioles to the alveolar ducts and alveolar spaces in the 1 and 3 mg-administered groups. Interstitial changes were also observed around these inflammatory changes 3 months after instillation.

We used PCM to evaluate collagen deposition in the lung tissues stained by the elastica van Gieson method, selecting the alveolar duct and pleura, where the initial deposition of collagen is often observed. In our previous study<sup>14)</sup>, we showed an increasing fibrogenic pattern of crystalline silica by PCM enhancing the collagen-positive sites through polarized light. Collagen deposition analysis using PCM could show the different patterns of collagen deposition in a time course after instillation of several sample materials.

In Fig. 4D, the image of lung in which P25 was instilled shows remarkable collagen depositions (bright areas) at the alveolar duct 6 months after instillation. Other images showed moderate collagen depositions at the similar location. The results of point counting showed that collagen deposition in the alveolar ducts was not cleared and the levels remained significantly high even 6 months after administration in the P25 group (Fig. 5B). Significant collagen deposition in the pleura was present only on the third day after administration (Fig. 5C). Significant changes were seen in the other groups, too, but were thought to be within the fluctuation range.

The Japan Society for Occupational Health finally recommended the occupational exposure limit of 0.3 mg/m<sup>3</sup> for TiO<sub>2</sub> nanoparticles<sup>25)</sup> based on the NOAEL of 2 mg/m<sup>3</sup>, which was reported by Bermudez et al.<sup>8)</sup> in a 13-week inhalation exposure test using P25. The results of this and previous studies indicated a relatively strong inflammatory reaction to P25, and thus it is likely that the above limit is on the safe side. Various surface modifications are used for TiO<sub>2</sub> nanoparticles depending on their applications, and such surface-modified particles have distinct properties. As shown in the present study, bridging studies where the results of intratracheal instillation of TiO<sub>2</sub> nanoparticles are compared with those of P25 will be effective for evaluating the biological effects of individual types of TiO<sub>2</sub> nanoparticles.

## Conclusion

It is generally thought that the pulmonary inflammation caused by nanoparticles increases when particle diameters become smaller and specific surface areas become larger, even with the same material. However, in this study, the most severe fibrosis was found in the P25 group, even though the BET the particle diameter was larger and the

specific surface area was smaller than other types of TiO<sub>2</sub> nanoparticles. Considering the differences in the crystal forms (rutile versus anatase) confirmed by X ray diffraction, the production methods and the characteristics of nanoparticles (e.g., mixed-crystal phase and amorphous) are likely to determine their biological effects. This study suggests that the surface area is not the only determinant of the toxicity of nanoparticles, and other factors, such as surface properties and synthetic methods, need to be taken into account when assessing the toxicity of nanoparticles.

*Acknowledgments:* This research was funded by a Grant-in-Aid for Scientific Research (No. 22590566) of the Japan Society for the Promotion of Science titled: “Pulmonary effect of titanium dioxide and various particles by instillation to rats: in relation to surface area dose metrics.”

*Conflicts of interest:* The authors have no conflicts of interest.

## References

- 1) Donaldson K, Brown D, Clouter A, et al. The pulmonary toxicology of ultrafine particles. *J Aerosol Med* 2002; 15(2): 213-220.
- 2) Christensen FM, Johnston HJ, Stone V, et al. Nano-TiO<sub>2</sub>-feasibility and challenges for human health risk assessment based on open literature. *Nanotoxicology* 2011; 5(2): 110-124.
- 3) The Essential Chemical Industry—online. [Online]. Available from: URL: <http://www.essentialchemicalindustry.org/chemicals/titanium-dioxide.html>
- 4) Wang WN, Lenggong W, Terashi Y, Kim TO, Okuyama K. One-step synthesis of titanium oxide nanoparticles by spray pyrolysis of organic precursors. *Materials Science and Engineering B* 2005; 123: 194-202.
- 5) Jiang J, Oberdörster G, Elder A, Gelein R, Mercer P, Biswas P. Does nanoparticle activity depend upon size and crystal phase? *Nanotoxicology* 2008; 2(1): 33-42.
- 6) Ferin J, Oberdorster G, Penney DP. Pulmonary retention of ultrafine and fine particles in rats. *Am J Respir Cell Mol Biol* 1992; 6(5): 535-542.
- 7) Baggs RB, Ferin J, Oberdörster G. Regression of pulmonary lesions produced by inhaled titanium dioxide in rats. *Vet Pathol* 1997; 34(6): 592-597.
- 8) Bermudez E, Mangum JB, Wong BA, et al. Pulmonary responses of mice, rats, and hamsters to subchronic inhalation of ultrafine titanium dioxide particles. *Toxicol Sci* 2004; 77: 347-357.
- 9) Warheit DB, Webb TR, Sayes CM, Colvin VL, Reed KL. Pulmonary instillation studies with nanoscale TiO<sub>2</sub> rods and dots in rats: toxicity is not dependent upon particle size and surface area. *Toxicol Sci* 2006; 91(1): 227-236.
- 10) Warheit DB, Webb TR, Reed KL, Frerichs S, Sayes CM. Pulmonary toxicity study in rats with three forms of ultrafine-TiO<sub>2</sub> particles: differential responses related to surface properties. *Toxicology* 2007; 230(1): 90-104.
- 11) Warheit DB. How to measure hazards/risks following exposures to nanoscale or pigment-grade titanium dioxide particles. *Toxicology Letters* 2013; 220: 193-204.
- 12) Brunauer S, Emmett PH, Teller E. Adsorption of gases in multimolecular layers. *J Am Chem Soc* 1938; 60: 309-319.
- 13) Oyabu T, Morimoto Y, Hirohashi M, et al. Dose-dependent pulmonary response of well-dispersed titanium dioxide nanoparticles following intratracheal instillation. *J Nanopart Res* 2013; 15: 1600, DOI 10.1007/s11051-013-1600-y.
- 14) Ogami A, Morimoto Y, Yamato H, Oyabu T, Kajiwara T, Tanaka I. Patterns of histopathological change determined by the point counting method and its application for the hazard assessment of respirable dust. *Inhal Toxicol* 2004; 16: 793-800.
- 15) Ogami A, Morimoto Y, Myojo T, et al. Histopathological changes in rat lung following intratracheal instillation of silicon carbide whiskers and potassium octatitanate whiskers. *Inhal Toxicol* 2007; 19: 753-758.
- 16) Ogami A, Yamamoto K, Morimoto Y, et al. Pathological features of rat lung following inhalation and intratracheal instillation of C<sub>60</sub> fullerene. *Inhal Toxicol* 2011; 23(7): 407-416.
- 17) Rushton EK, Jiang J, Leonard SS, et al. Concept of assessing nanoparticle hazards considering nanoparticle dosimetric and chemical/biological response metrics. *J Toxicol Environ Health Part A* 2010; 73: 445-461.
- 18) Sweeney S, Berhanu D, Ruenraroengsak P, et al. Nanotitanium dioxide bioactivity with human alveolar type-I-like epithelial cells: Investigating crystalline phase as a critical determinant. *Nanotoxicology* 2015; 9(4): 482-492.
- 19) Zaqout MS, Sumizawa T, Igisu H, Higashi T, Myojo T. Binding of human serum proteins to titanium dioxide particles in vitro. *J Occup Health* 2011; 53(2): 75-83.
- 20) Höhr D, Steinfartz Y, Schins RP, et al. The surface area rather than the surface coating determines the acute inflammatory response after instillation of fine and ultrafine TiO<sub>2</sub> in the rat. *Int J Hyg Environ Health* 2002; 205(3): 239-244.
- 21) Rehn B, Seiler F, Rehn S, Bruch J, Maier M. Investigations on the inflammatory and genotoxic lung effects of two types of titanium dioxide: untreated and surface treated. *Toxicol Appl Pharmacol* 2003; 189(2): 84-95.
- 22) Bonner JC, Silva RM, Taylor AJ, et al. Interlaboratory evaluation of rodent pulmonary responses to engineered nanomaterials: The NIEHS Nano GO Consortium. *Environ Health Perspect* 2013; 121(6): 676-682.
- 23) Kobayashi N, Naya M, Endoh S, Maru J, Yamamoto K, Nakanishi J. Comparative pulmonary toxicity study of nano-TiO<sub>2</sub> particles of different sizes and agglomerations in rats: different short- and long-term post-instillation results. *Toxicology* 2009; 264(1-2): 110-118.
- 24) Kajiwara T, Ogami A, Yamato H, Oyabu T, Morimoto Y, Tanaka I. Effect of particle size of intratracheally instilled crystalline silica on pulmonary inflammation. *J Occup Health* 2007; 49: 88-94.
- 25) The Japan Society for Occupational Health. Recommendation of Occupational Exposure Limits (2015-2016). *J Occup Health* 2015; 57: 394-417.